

Low-Energy $E1$ Strength Distributions of ^{68}Ni

N. N. Arsenyev^{a,*}, A. P. Severyukhin^{a,b}, V. V. Voronov^a, and Nguyen Van Giai^c

^aJoint Institute for Nuclear Research, Dubna, Moscow region, 141980 Russia

^bDubna State University, Dubna, Moscow region, 141982 Russia

^cInstitut de Physique Nucléaire, CNRS-IN2P3, Université Paris-Sud, F-91406 Orsay Cedex, France

*e-mail: arsenyev@theor.jinr.ru

Received March 4, 2019; revised March 20, 2019; accepted March 29, 2019

Abstract—We study the effects of the coupling between one- and two-phonon components of the wave functions on the low-energy electric dipole response of ^{68}Ni in a microscopic model based on an effective Skyrme interaction SLy5. The finite rank separable approach for the quasiparticle random phase approximation is used. The effect of phonon-phonon coupling leads to the fragmentation of the $E1$ strength to a lower energy and improves the agreement with available experimental data.

DOI: 10.1134/S1063779619050034

INTRODUCTION

Recently, with the advent of advanced radioactive beam facilities and novel experimental techniques, unexplored regions of exotic nuclei and new phenomena became accessible for detailed spectroscopic studies. The electric dipole ($E1$) response of nuclei at energies around particle separation energy is presently attracting much attention, particularly for unstable neutron-rich nuclei produced as radioactive beams [1]. The structure and dynamics of the low-energy dipole strength, also referred to as pygmy dipole resonance (PDR), has extensively been investigated using a variety of theoretical approaches and models; see, e.g., [2, 3]. In analogy to the giant dipole resonance (GDR), the PDR has been interpreted as a collective oscillation of the neutron skin with respect to a $N \approx Z$ inert core. The total sum of the measured energy-weighted sum rule (EWSR) of such $E1$ distributions is less than 1–2% of the Thomas–Reiche–Kuhn (TRK) sum rule value for stable nuclei and less than 5–6% for unstable neutron-rich nuclei [1]. The existence of the PDR mode near the neutron threshold has important astrophysical implications. The PDR study is expected to provide information on the symmetry energy term of the nuclear equation of state [3], is such an example.

A description of the properties of the low-energy $E1$ strength distribution requires the including of the coupling between one- and two-phonon components of the wave functions [4, 5]. The quasiparticle random phase approximation (QRPA) with a self-consistent mean-field derived from a Skyrme energy density functionals (EDF) is one of the most successful methods for studying the low-energy dipole strength, see e.g., [2, 3]. The main difficulty is that the complexity

of calculations beyond standard QRPA increases rapidly with the size of the configuration space, so that one has to work within limited spaces. By making use of the finite rank separable approximation (FRSA) [6, 7] for the residual interaction, one can perform Skyrme-QRPA calculations in very large two-quasiparticle spaces. Following the basic ideas of the quasiparticle-phonon model (QPM) [5], the FRSA has been generalized for the phonon–phonon coupling (PPC) [8]. The so-called FRSA was thus used to study the electric low-energy excitations and giant resonances within and beyond the Skyrme-QRPA [8–10]. In particular, we have applied the FRSA approach for calculating the PDR strength distribution [11, 12]. In this paper, we discuss the PPC effect on the $E1$ response for the unstable neutron-rich nucleus ^{68}Ni , focusing on the emergence and the properties of the PDR. There are ambiguous experimental data for the properties of the PDR in ^{68}Ni [13–15]. In particular, the observed centroid (\bar{E}_c) of the PDR varies from 9.55 ± 0.17 MeV [14] to 11 MeV [13] in the different experiments, exhausting respectively $2.8 \pm 0.5\%$ and $5.0 \pm 1.5\%$ of the $E1$ EWSR. Thus, ^{68}Ni nucleus is ideal candidate for such a study.

BRIEF OUTLINE OF THE METHOD

The method has been discussed in detail in [6, 7, 11] however we recall it for completeness. The Hartree–Fock–BCS (HF-BCS) calculations are performed by using the SLy5 EDF [16] in the particle-hole channel and a density-dependent zero-range interaction in the particle-particle channel. Spherical symmetry is assumed for the ground states. The continuous part of the single-particle spectrum is discretized by diago-

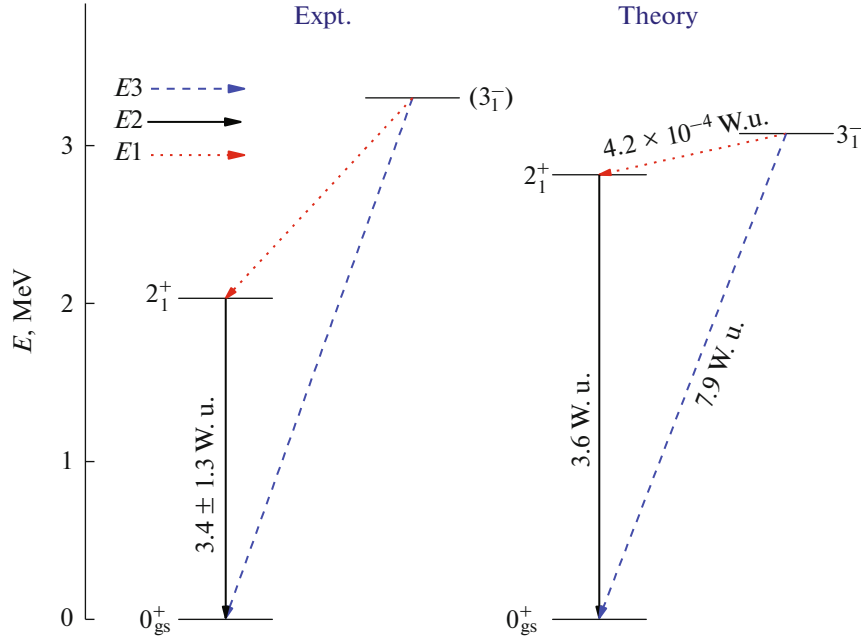


Fig. 1. Experimental [19, 20] and theoretical energies and transition probabilities of the $[2_1^+]_{\text{QRPA}}$ and $[3_1^-]_{\text{QRPA}}$ states for ^{68}Ni . The $B(E1; \downarrow)$, $B(E2; \downarrow)$, and $B(E3; \downarrow)$ factors are given in Weisskopf units (W.u).

nalizing the HF Hamiltonian in a harmonic oscillator basis. The strength of the zero-range volume force is taken equal to -270 MeV fm^3 in connection with the soft cutoff at 10 MeV above the Fermi energy as introduced in [7]. This value of the pairing strength is fitted to reproduce the experimental neutron pairing gaps of $^{50,52,54}\text{Ca}$ obtained by the three-point formula [7, 11]. This choice of the pairing interaction has also been used for a satisfactory description of the experimental data of $^{70,72,74,76}\text{Ni}$ [17], $^{90,92}\text{Zr}$ and $^{92,94}\text{Mo}$ [9]. The residual interaction in the particle-hole channel and in the particle-particle channel can be obtained as the second derivative of the EDF with respect to the particle density and the pair density, accordingly. By means of the standard procedure [18] we obtain the familiar QRPA equations in the configuration space. The eigenvalues of the QRPA equations are found numerically as the roots of a relatively simple secular equation within the FRSA [6]. Since the FRSA enables to us to use a large space, there is no need to introduce effective charges. The cutoff of the discretized continuous part of the single-particle spectra is at the energy of 100 MeV. This is sufficient to exhaust practically all the sum rules and, in particular, the classical TRK sum rule with the enhancement factor $\kappa = 0.25$ for the SLy5 EDF [16]. In the case of ^{68}Ni , the $E1$ strength distribution is well studied experimentally up to 28.4 MeV [14]. The total dipole strength is calculated in the 12–28.4 MeV interval, which exhausts 114% of the TRK sum rule within the PPC. The experimental data suggest the TRK value of $98 \pm 7\%$ [14].

To take into account the effects of the PPC we follow the basic QPM ideas [5]. We construct the wave functions of excited states from a linear combination of one- and two-phonon configurations as

$$\Psi_{\nu}(JM) = \left(\sum_i R_i(J\nu) Q_{JM_i}^+ + \sum_{\substack{\lambda_1 \mu_1 \\ \lambda_2 \mu_2}} P_{\lambda_2 \mu_2}^{\lambda_1 \mu_1}(J\nu) [Q_{\lambda_1 \mu_1}^+ Q_{\lambda_2 \mu_2}^+]_{JM} \right) |0\rangle, \quad (1)$$

where $Q_{\lambda \mu}^+ |0\rangle$ is the QRPA excitation having energy $\omega_{\lambda \mu}$; λ denotes the total angular momentum and μ is its z -projection in the laboratory system. The ground state is the QRPA phonon vacuum $|0\rangle$. The unknown amplitudes $R_i(\lambda\nu)$, $P_{\lambda_2 \mu_2}^{\lambda_1 \mu_1}(\lambda\nu)$ and the excited state energies E_{ν} are determined from the variational principle which leads to a set of linear equations [8, 9]. The equations have the same form as in the QPM [5], but the single-particle spectrum and the parameters of the residual interaction are obtained from the chosen Skyrme EDFs without any further adjustments.

In order to construct the wave functions (1) of the 1^- states, in the present study we take into account all two-phonon terms that are constructed from the phonons with multiplicities $\lambda \leq 5$ [11, 12]. As an example the energies and reduced transition probabilities of the first 2^+ and 3^- phonons for ^{68}Ni are presented in Fig. 1. The QRPA results obtained with the SLy5 EDF are compared with the experimental data [19, 20]. The $E1$ transition matrix elements are calculated with the

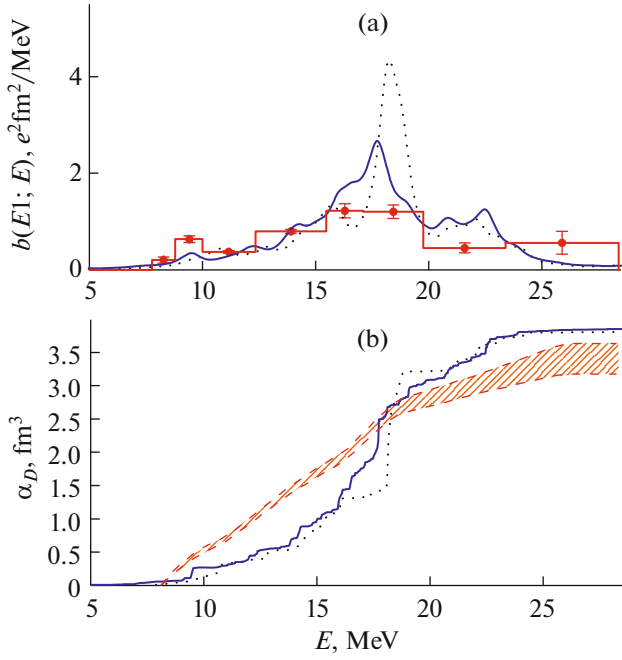


Fig. 2. (a) The experimental data of $E1$ strength distributions for ^{68}Ni (histogram and data points) are taken from [14]. The dotted and solid lines correspond to the calculations within the QRPA with the SLy5 EDF and taking into account the PPC, respectively. (b) Running sum of the electric dipole polarizability for ^{68}Ni calculated within the QRPA (dotted line) and the QRPA plus PPC (solid line) in comparison to experimental determination of α_D (the two dashed lines indicate upper and lower limits).

effective neutron, $e_{(\text{eff})}^{(n)} = -\frac{Z}{A}e$, and proton, $e_{(\text{eff})}^{(p)} = \frac{N}{A}e$, charges. As one can see, the overall agreement of the energies and $B(E\lambda; \downarrow)$ values with the data looks reasonable. For the wave function (1) of the 1^- states we include all one-phonon dipole states with energies below 35 MeV and 15 most collective phonons of other multipolarities (2^+ , 3^- , 4^+ and 5^-). The effect of configuration space extension on the results was tested and its minor role was found.

RESULTS AND DISCUSSION

As the first step in the present analysis, we discuss the GDR energy region. The experimental spectra is displayed in Fig. 2a. The histogram and data points are experimental data up to 28.4 MeV [14]. The calculated $E1$ strength distribution is computed by using a Lorentzian smearing with an averaging parameter $\Delta = 1.0$ MeV. The PPC effects yield a noticeable redistribution of the GDR strength in comparison with the QRPA results. It is worth mentioning that the coupling increases the GDR width from 6.2 to 6.8 MeV calcu-

lated for the energy interval 12–28.4 MeV. Also, the PPC induces a 100-keV downward shift of the GDR energy ($\bar{E}_c = 18.5$ MeV within the QRPA, which is analogous to other models [21]). The experimental GDR width and energy are 6.1 ± 0.5 MeV and 17.1 ± 0.2 MeV [14], respectively. The calculated characteristics of the GDR are in agreement with the observed values. The general shapes of the GDR obtained in the PPC are rather close to those observed in experiment. This demonstrates the improvement of the PPC description in comparison with QRPA.

In order to perform further investigations on the ^{68}Ni nucleus we have extracted the electric dipole polarizability (α_D), which represents a handle to constrain the equation of state of neutron matter and the physics of neutron stars [3]. The electric dipole polarizability α_D is defined as

$$\alpha_D = \frac{8\pi}{9} \sum_{\nu} B(E1; 0_{gs}^+ \rightarrow 1_{\nu}^-) / E_{1\nu}. \quad (2)$$

Running sums of the α_D value for ^{68}Ni in the energy region below 28.4 MeV are given in Fig. 2b. It is shown that the PPC insignificantly affects the distribution of the electric dipole polarizability near the localization of the GDR. However, the calculated values of α_D obtained by integrating the $E1$ strength up to the upper experimental limit are similar. Both calculations within the QRPA with the SLy5 EDF ($\alpha_D = 3.81 \text{ fm}^3$) and taking into account the PPC ($\alpha_D = 3.85 \text{ fm}^3$) reproduce the experimental data $\alpha_D = 3.40 \pm 0.23 \text{ fm}^3$ [14]. Although the GDR strength dominates, contributions to α_D value at lower and higher excitation energies must be taken into account.

Finally, let us now discuss the low-energy $E1$ strength. Using the analysis of the transition densities we found that the 1^- states below 12 MeV have the proton and neutron densities in the nuclear interior region are in phase. The neutron transition densities of these states are dominated outside the nuclear surface. That corresponds to the vibrations of a neutron skin against a proton-neutron core. Increasing further the excitation energy we observe the transition densities of an intermediate behavior or characterizing of the low-energy GDR tail. In QRPA calculations we recognize the centroid energy, \bar{E}_c , of the PDR is 10.6 MeV. Taking into account the PPC gives rise to a decrease of the PDR energy by 350-keV, while the observed centroid of the PDR varies from 9.55 ± 0.17 MeV [14] to 11 MeV [13]. The total dipole strength is $1.0 \text{ e}^2\text{fm}^2$ within the QRPA and $1.1 \text{ e}^2\text{fm}^2$ for the PPC. We find that the PDR contribution to the α_D value is 9.8% within the QRPA and 11.6% in the case of the QRPA plus PPC. The summation includes the dipole states below 12 MeV. The PPC calculations give an integrated energy-weighted $E1$ strength of the PDR is

4.6% of the TRK sum rule. These characteristics are in agreement with those extracted from the recent experimental data reported in [13–15]. Finally, the inclusion of the two-phonon terms results in an increase of the pygmy $E1$ -resonance width from 1.9 to 3.6 MeV. Recently measurement of the PDR in ^{68}Ni above the neutron emission threshold give the PDR width of 2 MeV [15]. A similar calculation has been performed for ^{68}Ni using the quasiparticle time blocking approximation (QTBA) in non-relativistic framework [22] and with relativistic Lagrangian (RQTBA) [23]. For comparison, the QTBA calculations give $\bar{E}_c = 10.8$ MeV [22]. In the case of the RQTBA, the calculated strength distribution in ^{68}Ni has its maximum at 10.3 MeV and the total strength below 12 MeV is $2.73 e^2\text{fm}^2$ [23].

SUMMARY

Starting from the Skyrme mean-field calculations, the properties of the $E1$ strength distribution of ^{68}Ni is studied by taking into account the coupling between one- and two-phonons terms in the wave functions. The finite-rank separable approach for the QRPA calculations enables one to reduce remarkably the dimensions of the matrices that must be inverted to perform nuclear structure calculations in very large configurational spaces. It is shown that the inclusion of the two-phonon configurations leads to an essential increase of the pygmy dipole resonance width of ^{68}Ni .

N.N.A., A.P.S., and V.V.V. thank the hospitality of INP-Orsay where a part of this work was done. This work was partly supported by the CNRS-RFBR grant no. 16-52-150003 and the IN2P3-JINR agreement.

REFERENCES

1. D. Savran, T. Aumann, and A. Zilges, “Experimental studies of the pygmy dipole resonance,” *Prog. Part. Nucl. Phys.* **70**, 210–245 (2013).
2. N. Paar, D. Vretenar, E. Khan, and G. Colò, “Exotic modes of excitation in atomic nuclei far from stability,” *Rep. Prog. Phys.* **70**, 691–793 (2007).
3. X. Roca-Maza and N. Paar, “Nuclear equation of state from ground and collective excited state properties of nuclei,” *Prog. Part. Nucl. Phys.* **101**, 96–176 (2018).
4. V. G. Soloviev, Ch. Stoyanov, and V. V. Voronov, “The influence of the giant dipole resonance on radiative strength functions in spherical nuclei,” *Nucl. Phys. A* **304**, 503–519 (1978).
5. V. G. Soloviev, *Theory of Atomic Nuclei: Quasiparticles and Phonons* (Institute of Physics, Bristol and Philadelphia, 1992).
6. N. V. Giai, Ch. Stoyanov, and V. V. Voronov, “Finite rank approximation for random phase approximation calculations with Skyrme interactions: An application to Ar isotopes,” *Phys. Rev. C* **57**, 1204–1209 (1998).
7. A. P. Severyukhin, V. V. Voronov, and N. V. Giai, “Effects of the particle-particle channel on properties of low-lying vibrational states,” *Phys. Rev. C* **77**, 024322 (2008).
8. A. P. Severyukhin, V. V. Voronov, and N. V. Giai, “Effects of phonon-phonon coupling on low-lying states in neutron-rich Sn isotopes,” *Eur. Phys. J. A* **22**, 397–403 (2004).
9. A. P. Severyukhin, N. N. Arsenyev, and N. Pietralla, “Proton-neutron symmetry in ^{92}Zr , ^{94}Mo with Skyrme interactions in a separable approximation,” *Phys. Rev. C* **86**, 024311 (2012).
10. A. P. Severyukhin, S. Åberg, N. N. Arsenyev, and R. G. Nazmitdinov, “Spreading widths of giant resonances in spherical nuclei: Damped transient response,” *Phys. Rev. C* **95**, 061305(R) (2017).
11. N. N. Arsenyev, A. P. Severyukhin, V. V. Voronov, and N. V. Giai, “Influence of complex configurations on the properties of the pygmy dipole resonance in neutron-rich Ca isotopes,” *Phys. Rev. C* **95**, 054312 (2017).
12. N. N. Arsenyev, A. P. Severyukhin, V. V. Voronov, and N. V. Giai, “Effects of 2 particle-2 hole configurations on dipole states in neutron-rich $N = 80-84$ isotones,” *Phys. Part. Nucl.* **48**, 876–878 (2017).
13. O. Wieland, et al., “Search for the pygmy dipole resonance in ^{68}Ni at 600 MeV/nucleon,” *Phys. Rev. Lett.* **102**, 092502 (2009).
14. D. M. Rossi, et al., “Measurement of the dipole polarizability of the unstable neutron-rich nucleus ^{68}Ni ,” *Phys. Rev. Lett.* **111**, 242503 (2013).
15. N. S. Martorana, et al., “First measurement of the isoscalar excitation above the neutron emission threshold of the pygmy dipole resonance in ^{68}Ni ,” *Phys. Lett. B* **782**, 112–116 (2018).
16. E. Chabanat, P. Bonche, P. Haensel, J. Meyer, and R. Schaeffer, “A Skyrme parametrization from subnuclear to neutron star densities. Part II: Nuclei far from stabilities,” *Nucl. Phys. A* **635**, 231–256 (1998).
17. A. P. Severyukhin, V. V. Voronov, I. N. Borzov, N. N. Arsenyev, and N. V. Giai, “Influence of $2p-2h$ configurations on β -decay rates,” *Phys. Rev. C* **90**, 044320 (2014).
18. J. Terasaki, J. Engel, M. Bender, J. Dobaczewski, W. Nazarewicz, and M. Stoitsov, “Self-consistent description of multipole strength in exotic nuclei: Method,” *Phys. Rev. C* **71**, 034310 (2005).
19. N. Bree, et al., “Coulomb excitation of $^{68}_{28}\text{Ni}_{40}$ at “safe” energies,” *Phys. Rev. C* **78**, 047301 (2008).
20. R. Broda, et al., “Spectroscopic study of the $^{64,66,68}\text{Ni}$ isotopes populated in $^{64}\text{Ni}+^{238}\text{U}$ collisions,” *Phys. Rev. C* **86**, 064312 (2012).
21. D. Vretenar, N. Paar, P. Ring, and G. A. Lalazissis, “Collectivity of the low-lying dipole strength in relativistic random phase approximation,” *Nucl. Phys. A* **692**, 496–517 (2001).
22. O. Achakovskiy, A. Avdeenkov, S. Goriely, S. Kamerdzhiev, and S. Krewald, “Impact of phonon coupling on the photon strength function,” *Phys. Rev. C* **91**, 034620 (2015).
23. E. Litvinova, P. Ring, and V. Tselyaev, “Relativistic two-phonon model for the low-energy nuclear response,” *Phys. Rev. C* **88**, 044320 (2013).